10-28-2018

Signature of Obliquity and Eccentricity in Soil Chronosequences

Christopher Shepard
University of Kentucky, Christopher.Shepard@uky.edu

Jon D. Pelletier
University of Arizona

Marcel G. Schaap
University of Arizona

Craig Rasmussen
University of Arizona

Digital Object Identifier (DOI)
https://doi.org/10.1029/2018GL078583

Geophysical Research Letters

RESEARCH LETTER
10.1029/2018GL078583

Key Points:
- A meta-analysis of soil chronosequences was used to analyze Quaternary soil preservation
- Quaternary soil preservation occurred at periodicities of 41 and 98 kyr, aligning with obliquity and eccentricity orbital cycles
- Quaternary soils predominantly date to periods of low rates of climatic change following rapid glacial-to-interglacial transitions

Supporting Information:
- Supporting Information S1
- Table S1

Correspondence to:
C. Shepard,
cbs8h@email.arizona.edu

Citation:
Shepard, C., Pelletier, J. D., Schaap, M. G., & Rasmussen, C. (2018). Signatures of obliquity and eccentricity in soil chronosequences. *Geophysical Research Letters, 45*, 11,147–11,153. https://doi.org/10.1029/2018GL078583

Received 1 MAY 2018
Accepted 8 SEP 2018
Accepted article online 12 SEP 2018
Published online 23 OCT 2018

Signatures of Obliquity and Eccentricity in Soil Chronosequences

Christopher Shepard[1,2], Jon D. Pelletier[3], Marcel G. Schaap[1], and Craig Rasmussen[1]

[1]Department of Soil, Water and Environmental Science, University of Arizona, Tucson, AZ, USA, [2]Department of Plant and Soil Sciences, University of Kentucky, Lexington, KY, USA, [3]Department of Geosciences, University of Arizona, Tucson, AZ, USA

Abstract Periodic shifts in Earth's orbit alter incoming solar radiation and drive Quaternary climate cycles. However, unambiguous detection of these orbitally driven climatic changes in records of terrestrial sedimentation and pedogenesis remains poorly defined, limiting our understanding of climate change-landscape feedbacks, impairing our interpretation of terrestrial paleoclimate proxies, and limiting linkages among pedogenesis, sedimentation, and paleoclimatic change. Using a meta-analysis, we show that Quaternary soil ages preserved in the modern record have periodicities of 41 and 98 kyr, consistent with orbital cycles. Further, soil ages predominantly date to periods of low rates of climatic change following rapid climate shifts associated with glacial-to-interglacial transitions. Soil age appears linked to orbital cycles via climate-modulated sediment deposition, which may largely constrain soil formation to distinct climate periods. These data demonstrate a record of widespread orbital cyclicity in sediment deposition and subsequent pedogenesis, providing a key insight into soil-landscape evolution and terrestrial paleo-environment changes.

Plain Language Summary Over the past 2.6 million years, the Earth's climate has cycled at regular intervals in concert with orbital variations. Climate variations have driven changes in the rates of erosion and deposition of new sediment, but detection of these orbitally driven climate cycles has remained elusive in soil systems. We demonstrated that soils were preserved to the present at the same intervals as known orbital climate cycles using a meta-analysis of soil chronosequences. We further tied dominant periods of soil formation to periods of relatively low rates of past climate change or periods of relatively stable, unchanging climate that enable soil formation. Our results provide a better understanding of how climate change impacts landscapes, which could greatly enhance our understanding of the impact of future climate change on soil resources and new insights into past environmental changes.

1. Introduction

The Quaternary climate system is controlled by a complex set of interactions among orbital forcings, oceanic circulation, and the terrestrial surface. Orbital climate control has been primarily documented in loess deposits (Ding et al., 1994), marine systems (Lisiecki & Raymo, 2005), and glacial systems (Abe-Ouchi et al., 2013; Jouzel et al., 2007; Lüthi et al., 2008). Quaternary climate variability was driven, in part, by periodicities in obliquity, precession, and eccentricity altering the amount of incoming solar radiation (Berger, 1988; Berger & Loutre, 1991; Imbrie & Imbrie, 1980) and the isostatic response of the lithosphere on the ice-albedo feedback (Abe-Ouchi et al., 2013). These records demonstrate the periodic dynamics of the Quaternary climate system and have hinted at the mechanisms controlling Quaternary climate variability. Apart from changes in incoming solar radiation, redistribution of heat and moisture from the poles toward the tropics via atmospheric and oceanic circulation patterns likely influences the amplitude and magnitude of past climate cycles (Jouzel et al., 2007; Lüthi et al., 2008) and likely influenced the transition from a Quaternary climate system dominated by the 41-kyr period to one dominated by the 100-kyr period at approximately 800 ka (Lisiecki, 2010). Further, Antarctic and global deuterium and carbon dioxide records (EPICA Dome C proxies) exhibit a tight coupling between global carbon dioxide concentrations and temperature throughout the Quaternary, with global temperatures slightly lagging carbon dioxide increases (Shakun et al., 2012). Existing paleoclimate records have provided significant advancements in understanding the Quaternary climate system, particularly with regard to marine and glacial systems, but extending this understanding

to terrestrial and pedogenic systems has been limited by the availability of relevant proxies (Pavich & Chadwick, 2004).

Soil formation and the climate system are tightly coupled (Ciais et al., 2013; Jenny, 1941) through CO_2 consumption in chemical weathering (Chadwick et al., 1994) and accumulation and stabilization of organic and inorganic forms of carbon (Harden et al., 1992; Schlesinger, 1982; Torn et al., 1997). Climate also modulates rates of sediment production and deposition, and soil-landscape evolution (Chadwick et al., 2013; White & Blum, 1995). Cooling and increased variability in the Quaternary climate system contributed to increased rates of erosion (Herman et al., 2013; Menounos et al., 2017; Zhang et al., 2001) with landscapes adjusting to changes in temperature, precipitation, and vegetation regimes (Langbein & Schumm, 1958; Menounos et al., 2017). These climatic changes drove large pulses of sediment redistribution from uplands to lowlands (Anders et al., 2005; Antinao et al., 2016; Bull & Schick, 1979; Owen et al., 2014) and eolian redistribution of sediments in periglacial areas (Ballantyne, 2002).

To date, little evidence of orbital cycles has been identified in either the direct soil-climate interaction through soil formation or its indirect form through deposition of soil parent material. One of the key obstacles to using soils as a proxy for orbitally driven climate change is the interaction between time and climate that influences soil property evolution (Pavich & Chadwick, 2004). Soil chronosequences record the approximate timing of initial soil formation from deposited parent materials (i.e., deposited sediment), providing a potential proxy of Quaternary climate cycling and sediment deposition. In the following, we demonstrate that a suitably broad meta-analysis of previously described soil chronosequence data sets reveals similar periodicities in soil preservation, climate, and orbital forcing. We hypothesized that soil age represents a terrestrial proxy for orbitally driven climate change and is indicative of the deposition of soil parent material relative to past climate cycles.

2. Methods

For the meta-analysis, we identified 41 distinct chronosequences and a total of 399 unique soil profiles that spanned a global array of modern climate systems, ecosystems, parent materials, and geomorphic landforms (Shepard et al., 2017; Table S1 and Figure S1). Eighty-six percent of the soils were located in depositional regimes, with the remaining 14% located in volcanic/tectonic regimes. Because tropical and southern hemisphere soils are underrepresented in the literature, most (84%) of the soils were from northern temperate latitudes (30°–60°N), which likely weights the presented results more heavily toward the paleoenvironmental changes in the northern hemisphere. Additionally, the chronosequence meta-analysis may suffer from bias due to selective sampling, and selective publication of available data. The most prevalent age dating methods included radiocarbon, landscape position, potassium-argon dating, and dendrochronology (Table S1). All presented analyses were carried out using the statistical software R (v. 3.1.1, www.r-project.org).

The soil ages ranged from 0.01 to 4,350 ka, with the vast majority younger than 1,000 ka (>90%; Figure 1a). Soils continually form in newly deposited sediment, with some proportion subsequently destroyed by erosive processes, such that the soil chronosequence database provides an approximation of the net number of soils preserved to the present. The cumulative soil age distribution can be represented with a cumulative exponential distribution (rate, $\lambda = 6.25$/kyr; Figure 1b), thus providing a probabilistic estimate of Quaternary soil preservation and an estimated soil half-life of 286 kyr (Griffiths, 1993). The soil half-life, calculated using the λ value, provides an estimate of the amount of time required for half of Quaternary soils to be removed from the Earth's surface.

2.1. Soil Age Time Series

To determine periodicity in soil age, we calculated a soil time series from the number of observed soils from the available chronosequence database (Shepard et al., 2017). Using a 10-kyr window, we calculated the temporal density of the number of soils preserved in 1-kyr increments from 0 to 2,600 ka. We weighted the number of observed soils, both 5 kyr older and younger than the target age (i.e., 10-kyr window), according to: 1.0, 0.5, 0.25, 0.125, and 0.0625. For example, if the target year was 20 ka, we calculated the temporal density of the number of soils from 15 to 25 ka. We summed the weighted number of observed soils within the 10-kyr window and divided by the size of the window (i.e., 10 kyr), repeating the calculation in 1-kyr increments. We calculated the temporal density in this manner to account for the uncertainty and lack of precise age

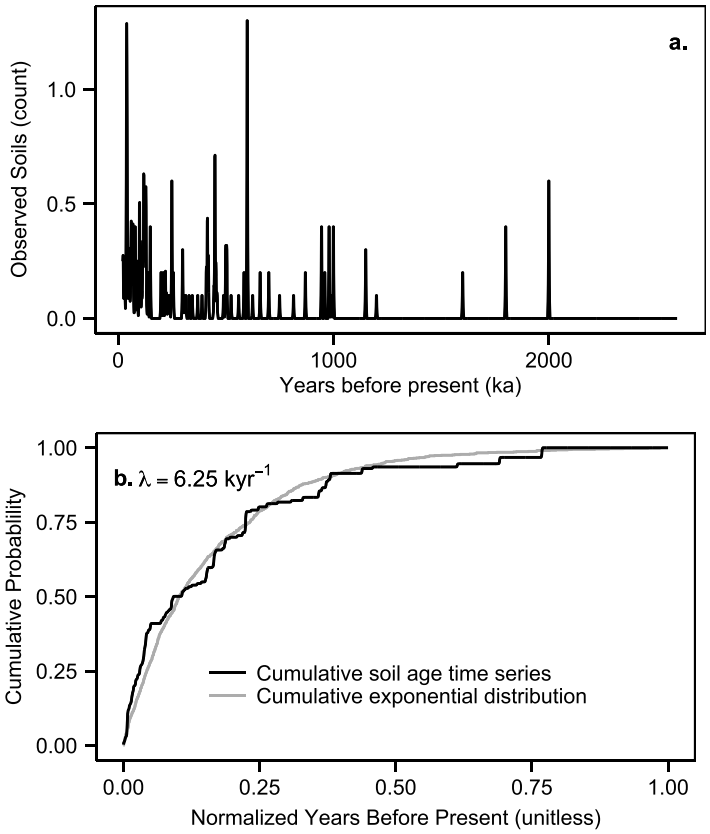

Figure 1. Soil age time series and cumulative distribution. (a) Soil age time series calculated from the number of preserved soils to the present in the soil chronosequence database (Shepard et al., 2017). (b) Cumulative probability distribution of the soil age time series fitted to a cumulative exponential distribution (rate, $\lambda = 6.25$/kyr) with normalized age.

constraint of soil age within the available chronosequence literature. From the soil age time series, we calculated a cumulative probability distribution from Last Glacial Maximum (~22 ka, LGM) to ~2,600 ka by cumulatively adding the soil age time series. We qualitatively fitted a cumulative exponential distribution to the cumulative soil age distribution.

We used the Lomb-Scargle (LS) periodogram to determine the periodicity in the soil age time series (Lomb, 1976; Scargle, 1982). The LS periodogram of the soil time series was calculated using the R package "lomb" (Ruf, 2015). We used an oversampling factor of 10, with a significance level of 0.05. We only examined the timing of Quaternary soil preservation from LGM (22 ka) to ~500 ka, and from LGM to the beginning of the Pleistocene (~2,600 ka), and periodicities between 10 and 200 kyr. We assumed that younger soils would not have experienced full climatic or orbital cycles; soils older than 500 ka have a sparse distribution, which could lead to spurious results. We used the LS periodogram because it provides a significance level and can handle unevenly sampled data. Significance levels were determined using the function "randlsp," which rearranges the data set to determine the probability that random peaks will reach or exceed the peaks of the original data set. We also calculated the LS periodogram for eccentricity, obliquity, and precession indices (Berger & Loutre, 1991); EPICA Dome C deuterium temperature (Jouzel et al., 2007) and CO_2 concentration records (Lüthi et al., 2008); and the LR04 Global Stack $\delta^{18}O$ record (Lisiecki & Raymo, 2005) to demonstrate correspondence between the soil age time series and paleoclimate proxy periodograms.

2.2. Paleoclimatic Proxies

We used available $\delta^{18}O$ (‰) records derived from marine carbonate sediment and speleothems as proxies for the general paleoclimate conditions and potential sediment denudation/production rates (Table S2). We chose these proxies as they have demonstrated linkages between paleoclimate conditions and orbital

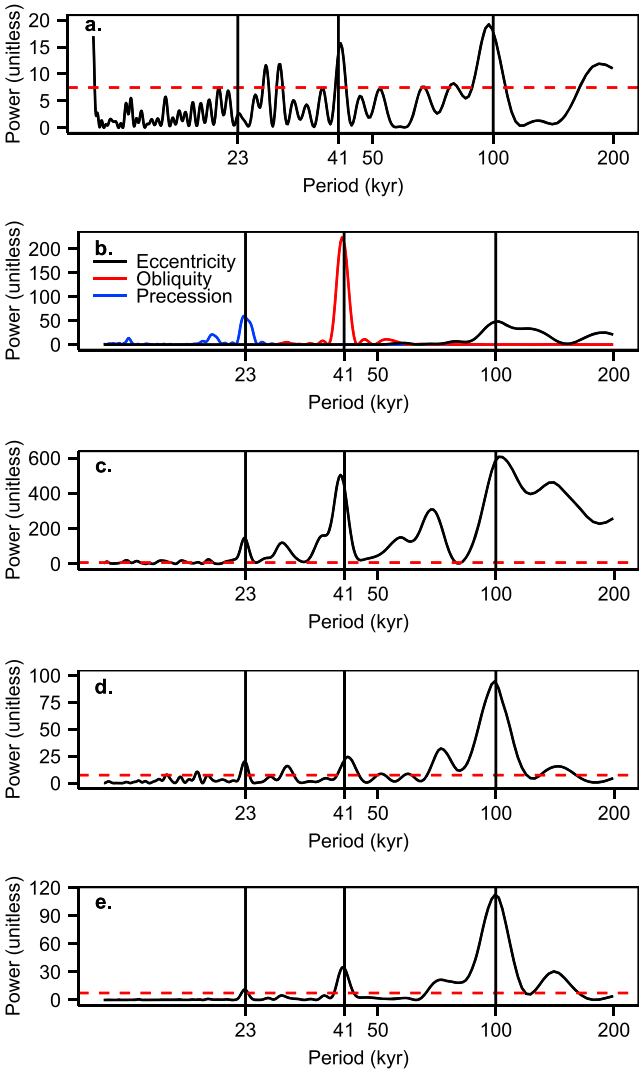

Figure 2. Lomb-Scargle periodograms of soil age time series and orbital and paleoclimate records. (a) Periodogram of the soil age time series of the number of preserved soil to the present from 500 to 22 ka, showing periodicities in soil preservation at 98 and 41 kyr. (b) Peridogram of eccentricity (black), obliquity (red), and precession index (blue) (Berger & Loutre, 1991). (c) Periodogram of EPICA Dome C deuterium temperature record (Jouzel et al., 2007). (d) Periodogram of EPICA Dome C CO_2 concentration record (Lüthi et al., 2008). (e) Periodogram for the LR04 Global Stack $\delta^{18}O$ record (Lisiecki & Raymo, 2005). The vertical bars indicate orbital precession (23 kyr), obliquity (41 kyr), and eccentricity (100 kyr) cycles; the red dashed lines represent *p*-value equal to 0.05.

forcing. We examined both the $\delta^{18}O$ record and the rate of change in the $\delta^{18}O$ values ($\Delta\delta^{18}O$). The rate of change in the $\delta^{18}O$ record ($\Delta\delta^{18}O$) was calculated as

$$\Delta\delta^{18}O\ (‰/kyr) = \frac{\delta^{18}O_{i+1} - \delta^{18}O_i}{time_{i+1} - time_i} \quad (1)$$

where $\delta^{18}O_i$ represents the $\delta^{18}O$ at the current time ($time_i$) and $\delta^{18}O_{i+1}$ represents the $\delta^{18}O$ at the preceding time ($time_{i+1}$) in the record; we used the $\Delta\delta^{18}O$ as a proxy for climate stability (Benson, 2004). Climate stability was defined as periods when the $\Delta\delta^{18}O$ was within $\pm2\sigma$ of the average $\Delta\delta^{18}O$, whereas climate instability was defined as periods in which $\Delta\delta^{18}O$ was outside of $\pm2\sigma$ of the average $\Delta\delta^{18}O$. We assumed that the $\delta^{18}O$ record broadly represents general patterns and shifts in global climate and temperature but not any specific local climate conditions.

The $\Delta\delta^{18}O$ and $\delta^{18}O$ values at the time of initial soil formation were determined by aligning the age of each soil to its approximate position in the $\delta^{18}O$ records, and the percentage of sites within $\pm2\sigma$ of the average $\Delta\delta^{18}O$ values was determined. If there was no influence between past climate change and soil formation, there would be an equal probability of observing soil ages at any value of $\Delta\delta^{18}O$, with an expected uniform distribution. The distributions of soil $\Delta\delta^{18}O$ values were tested against an expected random uniform distribution using the chi-square goodness of fit test. We also tested the distribution of soil $\Delta\delta^{18}O$ values against a normal distribution. For the percentage of soil $\Delta\delta^{18}O$ values within $\pm2\sigma$ of the average $\Delta\delta^{18}O$ an ordinary bootstrap was used to determine normal 95% confidence intervals. We determined the number of soil ages dating to either glacial or interglacial marine isotope stages, and used a chi square test, assuming an equal split in soil ages between glacial and interglacial stages, to determine the significance of the observed distribution of glacial and interglacial soil ages.

3. Results and Discussion

Using the LS periodogram analysis on soil ages from 22 to 500 kyr and a 95% confidence level, we can identify peaks at 41 and 98 kyr (Figure 2a), with the strongest periodicity at 98 kyr ($p < 0.0001$). Additional peaks were observed at 27 and 29 kyr (Figure 2a). A periodogram based on an extended period with soil ages between 22 ka to 2,600 ka yielded qualitatively similar results (Figure S2) but with a decreased peak near 100 kyr and increased peaks near 41 and 50 kyr, consistent with the relatively smaller 100-kyr forcing of the early Pleistocene (Lisiecki, 2010). Observed soil age periodicities aligned with observed eccentricity and obliquity but did not exhibit a compelling signature of precession (23 kyr; Figure 2b; Berger & Loutre, 1991). The soil age periodicities near 41 and 98 kyr align with periodicities in the EPICA Dome C deuterium temperature (Figure 2c; Jouzel et al., 2007) and CO_2 concentration records (Figure 2d; Lüthi et al., 2008) and the LR04 Global Stack $\delta^{18}O$ proxy (Figure 2e, Lisiecki & Raymo, 2005). In addition, the soil age periodicities at 27 and 29 kyr align with peaks in the deuterium and CO_2 record but not with LR04 $\delta^{18}O$ record. These results demonstrate that there is a correspondence in periodicities among orbital cycles, global climate cycles, and soil formation and preservation in depositional regimes throughout the Pleistocene.

We compared the timing of potential initial soil formation to rates of change in the available paleoclimate proxies to better understand the conditions under which the general paleoclimate state may promote the observed periodicities in the soil age time series. We found the rate of past climate change corresponded

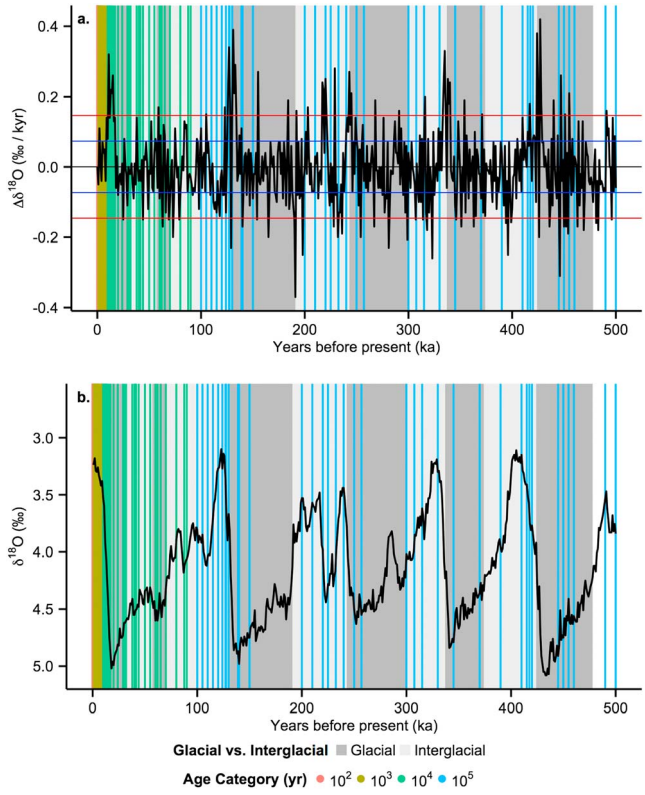

Figure 3. Time of soil formation related to the LR04 Stack $\delta^{18}O$ record (Lisiecki & Raymo, 2005). Soil ages preferentially grouped around relatively stable interglacial stages. The colored vertical lines represent the age of each soil in the chronosequence database (Shepard et al., 2017) categorized into order of magnitude categories, from 10^2 to 10^5 years; the dark gray bars represent glacial isotope stages, and the lighter gray bars represent interglacial isotope stages. (a) Rate of change of $\delta^{18}O$ record from 0 to 500 ka ($\Delta\delta^{18}O$); the black horizontal line represents the mean rate, the blue horizontal line represents $\pm1\sigma$ of $\Delta\delta^{18}O$, and the red horizontal line represents $\pm2\sigma$ of $\Delta\delta^{18}O$. (b) LR04 Stack $\delta^{18}O$ record from 0 to 500 ka.

with the initiation of soil formation and parent material deposition, with soil ages largely dating to periods of low relative climate change immediately following large climate shifts. Depending on the paleoclimate record, 87–98% of pre-Last Glacial Maximum (>22 ka, pre-LGM) soils formed at a time when the rate of change in $\delta^{18}O$ ($\Delta\delta^{18}O$; equation (1)) was within $\pm2\sigma$ of the average $\Delta\delta^{18}O$ across the included paleoclimate proxies (Figure 3a and Table S2). Across all records, the distribution of $\Delta\delta^{18}O$ values at time of initial soil formation was statistically different from either expected uniform or normal distributions using a chi-square goodness of fit test (Table S2). Based on the LR04 stack marine isotope stages (Lisiecki & Raymo, 2005), almost equal time was observed between cooling and warming climates during the Pleistocene, with 1,294 kyr characterized by a cooling climate, indicative of "glacial" marine isotope stages (49.8%), and 1,306 kyr characterized by a warming climate, indicative of "interglacial" marine isotope stages (50.2%). In comparison, 63% of pre-LGM soil ages corresponded with interglacial climate periods, compared to 37% that occurred during glacial climate periods (chi-square test, $p < 0.001$; Figure 3b); of the soils dating to glacial periods, 35% were formed by tectonic/volcanic processes, with the remainder of soil ages occurring during or just preceding glacial-to-interglacial transitions (Figure S3).

The connection among orbital cycles, global climate change, and soil age distribution is likely driven by climate change effects on sediment redistribution and landscape stability. Sediment pulses are often driven by climate change (Anders et al., 2005; Antinao et al., 2016; Bull & Schick, 1979), such that periods of rapidly changing climate leads to increased erosion and sediment deposition. Soils preserved to the present, representing the net result of soils forming from these sediment pulses and soils removed via erosion, would thus propagate this climate signal into their age structure. A similar link was previously shown in stratigraphic records (Abdul Aziz et al., 2008; Ding et al., 1994), but to our knowledge has not been demonstrated in extant surface soils. As similar to other terrestrial climate records, the periodicity in the soil age time series does not exactly match Milankovitch orbital climate cycles (Pavich & Chadwick, 2004). This may be due to nonlinear responses in vegetation communities, precipitation regime change, glacial retreat, sea-level rise, and sediment production (Bard et al., 1996; Davis & Shaw, 2001; Ding et al., 1994).

Soils were preserved at orbital periodicities, predominantly date to periods of relatively low rates of climate change, and exhibited an exponential age distribution reflecting a balance of soil formation and erosion. The orbital periodicity in soil age clearly reflects interactions among global climate dynamics, erosion rates, and soil formation processes, representing a proxy for orbitally driven climate change. Sediment pulses triggered by punctuated periods of rapid climate change during orbitally driven glacial-to-interglacial transitions (Abe-Ouchi et al., 2013) likely drove increased sediment deposition (Zhang et al., 2001). Rapidly changing climate conditions of glacial-interglacial transitions likely do not allow significant soil formation to occur. The deposited sediment eventually served as the parent material for many soils (Anders et al., 2005) with soil formation preferentially occurring during the relatively more stable climate of interglacial periods, tying soil ages to orbital climate cycles. Further, interactions among warmer interglacial periods, global increase in vegetation, and deposited sediment may have facilitated more stabilized surfaces for soils to form on. Additionally, changes in drainage patterns and direction of sedimentation may influence soil preservation and the propagation of the orbital climate signal in the soil ages (Foreman & Straub, 2017). Soil formation in deposited sediment and deglaciated terrestrial areas draws down CO_2 from the atmosphere through organic carbon stabilization (Harden et al., 1992; Torn et al., 1997), chemical weathering (Chadwick et al., 1994), and pedogenic carbonate accumulation (Schlesinger, 1982), with the greatest rates of carbon

stabilization and storage occurring between 10^4 and 10^5 years (Torn et al., 1997), equivalent with the time scale of Quaternary climate cycles. The CO_2 consumed in soil formation processes, following sediment deposition after glacial-interglacial transitions, may in part facilitate the return to full glacial conditions by capturing atmospheric CO_2, in concert with orbital forcing and other climate feedbacks (Brovkin et al., 2012; Lüthi et al., 2008). The regular periodicities of soil ages coincident with orbital cycles provide a global explanation for the regular periods of observed soil formation (Morrison, 1964), and this work represents one of the first orbital interpretations of terrestrial paleoclimate records.

Acknowledgments
We thank Kristie Gallardo, Molly van Dop, and Irma Perez for help in extracting chronosequence data for this study. Support for C. S. came from the University Fellows program at the University of Arizona and the University of Arizona/NASA Space Grant Graduate Fellowship. This research was funded by the U.S. National Science Foundation grant EAR-1331408 in support of the Santa Catalina-Jemez River Basin Critical Zone Observatory. All data are available from the references included in Tables S1 and S2, and as cited. The authors have no conflicts of or competing interests.

References

Abdul Aziz, H., Hilgen, F. J., van Luijk, G. M., Sluijs, A., Kraus, M. J., Pares, J. M., & Gingerich, P. D. (2008). Astronomical climate control on paleosol stacking patterns in the upper Paleocene-lower Eocene Willwood Formation, Bighorn Basin, Wyoming. *Geology*, *36*(7), 531–534. https://doi.org/10.1130/G24734A.1

Abe-Ouchi, A., Saito, F., Kawamura, K., Raymo, M. E., Okuno, J., Takahashi, K., & Blatter, H. (2013). Insolation-driven 100,000 cycles and hysteresis of ice-sheet volume. *Nature*, *500*(7461), 190–193. https://doi.org/10.1038/nature12374

Anders, M. D., Pederson, J. L., Rittenour, T. M., Sharp, W. D., Gosse, J. C., Karlstrom, K. E., et al. (2005). Pleistocene geomorphology and geochronology of eastern Grand Canyon: Linkages of landscape components during climate change. *Quaternary Science Reviews*, *24*, 2428–2448.

Antinao, J. L., McDonald, E., Rhodes, E. J., Brown, N., Barrera, W., Gosse, J. C., & Zimmerman, S. (2016). Late Pleistocene-Holocene alluvial stratigraphy of southern Baja California, Mexico. *Quaternary Science Reviews*, *146*, 161–181. https://doi.org/10.1016/j.quascirev.2016.06.008

Ballantyne, C. K. (2002). Paraglacial geomorphology. *Quaternary Science Reviews*, *21*(18-19), 1935–2017. https://doi.org/10.1016/S0277-3791(02)00005-7

Bard, E., Hamelin, B., Arnold, M., Montaggioni, L., Cabiochi, G., Faure, G., & Rougerie, F. (1996). Deglaical sea-level record from Tahiti corals and the timing of global meltwater discharge. *Nature*, *382*(6588), 241–244. https://doi.org/10.1038/382241a0

Benson, L. (2004). Western lakes. In A. R. Gillespie, S. C. Porter, & B. F. Atwater (Eds.), *The Quaternary period of the United States* (pp. 185–204). Amsterdam, ND: Elseiver.

Berger, A. (1988). Milankovitch theory and climate. *Reviews of Geophysics*, *26*(4), 624–657. https://doi.org/10.1029/RG026i004p00624

Berger, A., & Loutre, M. F. (1991). Insolation values for the climate of the last 10 million years. *Quaternary Science Reviews*, *10*(4), 297–317. https://doi.org/10.1016/0277-3791(91)90033-Q

Brovkin, V., Ganopolski, A., Archer, D., & Munhoven, G. (2012). Glacial CO_2 cycle as a succession of key physical and biogeochemical processes. *Climate of the Past*, *8*(1), 251–264. https://doi.org/10.5194/cp-8-251-2012

Bull, W. B., & Schick, A. P. (1979). Impact of climatic change on an arid watershed: Nahal Yael, southern Israel. *Quaternary Research*, *11*(02), 153–171. https://doi.org/10.1016/0033-5894(79)90001-2

Chadwick, O. A., Kelly, E. F., Merritts, D. M., & Amundson, R. G. (1994). Carbon dioxide consumption during soil development. *Biogeochemistry*, *24*, 115–127.

Chadwick, O. A., Roering, J. J., Heimsath, A. M., Levick, S. R., Asner, G. P., & Khomo, L. (2013). Shaping post-orogenic landscapes by climate and chemical weathering. *Geology*, *41*(11), 1171–1174. https://doi.org/10.1130/G34721.1

Ciais, P., Sabine, C., Bala, B., Bopp, L., Brovkin, V., Canadell, J., et al. (2013). Carbon and other biogeochemical cycles. In T. F. Stocker, Q. Din, G.-K. Plattner, M. Tignor, S. K. Allen, J. Boschung, et al. (Eds.), *Climate change 2013: The physical basis. Contribution of Working Group I to the Fifth Assessment Report of the Intergovernmental Panel on Climate Change* (pp. 465–570). Cambridge, UK: Cambridge University Press.

Davis, M. B., & Shaw, R. G. (2001). Range shifts and adaptive responses to Quaternary climate change. *Science*, *292*(5517), 673–679. https://doi.org/10.1126/science.292.5517.673

Ding, Z., Yu, Z., Rutter, N. W., & Liu, T. (1994). Toward an orbital time scale for Chinese loess deposits. *Quaternary Science Reviews*, *13*(1), 39–70. https://doi.org/10.1016/0277-3791(94)90124-4

Foreman, B. Z., & Straub, K. M. (2017). Autogenic geomorphic processes determine the resolution and fidelity of terrestrial paleoclimate records. *Science Advances*, *3*(9), e1700683. https://doi.org/10.1126/sciadv.1700683

Griffiths, G. A. (1993). Estimation of landform life expectancy. *Geology*, *21*(5), 403–406. https://doi.org/10.1130/0091-7613(1993)021<0403:EOLLE>2.3.CO;2

Harden, J. W., Sunquist, E. T., Stallard, R. F., & Mark, R. K. (1992). Dynamics of soil carbon during deglaciation of the Laurentide ice sheet. *Science*, *258*(5090), 1921–1924. https://doi.org/10.1126/science.258.5090.1921

Herman, F., Seward, D., Valla, P. G., Carter, A., Kohn, B., Willett, S. D., & Ehlers, T. A. (2013). Worldwide acceleration of mountain erosion under a cooling climate. *Nature*, *504*(7480), 423–426. https://doi.org/10.1038/nature12877

Imbrie, J., & Imbrie, J. Z. (1980). Modeling the climatic response to orbital variations. *Science*, *207*(4434), 943–953. https://doi.org/10.1126/science.207.4434.943

Jenny, H. (1941). *Factors of soil formation: A system for quantitative pedology*. New York: Dover Publications, Inc.

Jouzel, J., Masson-Delmotte, V., Cattani, O., Dreyfus, G., Falourd, S., Hoffmann, G., et al. (2007). Orbital and millennial Antarctic climate variability over the past 800,000 years. *Science*, *317*(5839), 793–796. https://doi.org/10.1126/science.1141038

Langbein, W. B., & Schumm, S. A. (1958). Yield of sediment in relation to mean annual precipitation. *Eos, Transactions American Geophysical Union*, *39*(6), 1076–1084. https://doi.org/10.1029/TR039i006p01076

Lisiecki, L. (2010). Links between eccentricity forcing and the 100,000-year glacial cycle. *Nature Geoscience*, *3*(5), 349–352. https://doi.org/10.1038/ngeo828

Lisiecki, L. E., & Raymo, M. E. (2005). A Pliocene-Pleistocene stack of 57 globaly distributed benthic $\delta^{18}O$ records. *Paleoceanography*, *20*, PA1003. https://doi.org/10.1029/2004PA001071

Lomb, N. R. (1976). Least-squares frequency analysis of unequally spaced data. *Astrophysics and Space Science*, *39*(2), 447–462. https://doi.org/10.1007/BF00648343

Lüthi, D., Le Floch, M., Bereiter, B., Blunier, T., Marnola, J. -M., Siegenthaler, U., et al. (2008). High-resolution carbon dioxide concentration record 650,000-800,000 years before present. *Nature*, *453*(7193), 379–382. https://doi.org/10.1038/nature06949

Menounos, B., Goehring, B. M., Osborn, G., Margold, M., Ward, B., Bond, J., et al. (2017). Cordilleran ice sheet mass loss preceded climate reversals near the Pleistocene termination. *Science*, *358*(6364), 781–784. https://doi.org/10.1126/science.aan3001

Morrison, R. B. (1964). *Lake Lahontan: Geology of southern Carson Desert, Nevada USGS Professional Paper 401*. Washington, DC: United States Government Printing Office.

Owen, L. A., Clemmens, S. J., Finkel, R. C., & Gray, H. (2014). Late Quaternary alluvial fans at the eastern end of the San Bernardino Mountains, Southern California. *Quaternary Science Reviews*, *87*, 114–134. https://doi.org/10.1016/j.quascirev.2014.01.003

Pavich, M. J., & Chadwick, O. A. (2004). Soils and the Quaternary climate system. In A. R. Gillespie, S. C. Porter, & B. F. Atwater (Eds.), *The Quaternary period of the United States* (pp. 311–330). Amsterdam, Netherlands: Elsevier.

Ruf, T. (2015). Package "lomb". CRAN.

Scargle, J. (1982). Studies in astronomical time series analysis. II—Statistical aspects of spectral analysis of unevenly spaced data. *The Astronomical Journal*, *263*, 835–853. https://doi.org/10.1086/160554

Schlesinger, W. H. (1982). Carbon storage in the caliche of arid soils: A case study from Arizona. *Soil Science*, *133*(4), 247–255. https://doi.org/10.1097/00010694-198204000-00008

Shakun, J. D., Clark, P. U., He, F., Marcott, S. A., Mix, A. C., Liu, Z., et al. (2012). Global warming preceded by increasing carbon dioxide concentrations during the last glaciation. *Nature*, *484*(7392), 49–54. https://doi.org/10.1038/nature10915

Shepard, C., Schaap, M. G., Pelletier, J. D., & Rasmussen, C. (2017). A probabilistic approach to quantifying soil physical properties via time-integrated energy and mass input. *The Soil*, *3*(1), 67–82. https://doi.org/10.5194/soil-3-67-2017

Torn, M., Trumbore, S., Chadwick, O., Vitousek, P., & Hendricks, D. (1997). Mineral control of soil organic carbon storage and turnover. *Nature*, *389*(6647), 170–173. https://doi.org/10.1038/38260

White, A. F., & Blum, A. E. (1995). Effects of climate on chemical weathering in watersheds. *Geochimica et Cosmochimica Acta*, *59*(9), 1729–1747. https://doi.org/10.1016/0016-7037(95)00078-E

Zhang, P., Molnar, P., & Downs, W. R. (2001). Increased sedimentation rates and grain sizes 2-4 Myr ago due to the influence of climate change on erosion rates. *Nature*, *410*, 891–897.